THE JOURNAL OF BIOLOGICAL CHEMISTRY

Vol. 259, No. 17, Issue of September 10, pp. 11001–11009, 1984
Printed in U.S.A.

Electron Spin Relaxation of Cu_A and Cytochrome *a* in Cytochrome *c* Oxidase

COMPARISON TO HEME, COPPER, AND SULFUR RADICAL COMPLEXES*

(Received for publication, April 3, 1984)

Gary W. Brudvig‡, David F. Blair§, and Sunney I. Chan¶

From the Arthur Amos Noyes Laboratory of Chemical Physics, California Institute of Technology, Pasadena, California 91125

The method of continuous saturation has been used to measure the electron spin relaxation parameter T_1T_2 at temperatures between 10 and 50 K for a variety of $S = ½$ species including: Cu_A and cytochrome *a* of cytochrome *c* oxidase, the type 1 copper in several blue copper proteins, the type 2 copper in laccase, inorganic Cu(II) complexes, sulfur radicals, and low spin heme proteins. The temperature dependence and the magnitude of T_1T_2 for all of the species examined are accounted for by assuming that the Van Vleck Raman process dominates the electron spin-lattice relaxation. Over the entire temperature range examined, the relaxation of the type 1 coppers is six to seven times faster than that of type 2 copper, inorganic copper, and sulfur radicals, in spite of the similar *g*-anisotropies of these species. This result may indicate that the coupling of the phonon bath to the spin center is more effective in type 1 coppers than in the other complexes studied. The relaxation of Cu_A of cytochrome oxidase exhibits an unusual temperature dependence relative to the other copper complexes studied, suggesting that the protein environment of this center is different from that of the other copper centers studied and/or that Cu_A is influenced by a magnetic dipolar interaction with another, faster-relaxing paramagnetic site in the enzyme. A comparison of the saturation characteristics of the Cu_A EPR signal in native and partially reduced CO complexes of the enzyme also suggests the existence of such an interaction. The implications of these results with respect to the disposition of the metal centers in cytochrome oxidase are discussed.

Two of the four metal centers in oxidized cytochrome *c* oxidase, cytochrome *a* and Cu_A, exhibit EPR signals (1). The Cu_A center has been observed to have unusual EPR saturation characteristics. At 77 K the EPR signal from the Cu_A center is relatively difficult to saturate (2), while at 10 K the EPR signal is more easily saturated (3, 4) than other Cu(II) complexes. This unusual EPR saturation behavior has not been explained, and it may be an indication that one of the two hemes in cytochrome *c* oxidase is close to the Cu_A center. However, the Cu_A center is unlike the Cu(II) sites found in other proteins (3–7), and it is possible that the EPR saturation properties of the Cu_A center derive from its unusual structure. On the basis of its unusual *g*-values (2.18, 2.03, and 1.99) and small copper hyperfine splitting, it has been proposed that the Cu_A center is best described as a Cu(I)-sulfur radical site in the oxidized enzyme (3). On the other hand, cytochrome *a* exhibits EPR parameters typical of low spin heme (7).

In this work we have investigated the electron spin relaxation properties of both cytochrome *a* and the Cu_A center by the method of continuous saturation. The data on the Cu_A center have been compared to the EPR saturation of several sulfur radicals as well as a number of copper proteins and inorganic copper complexes. In addition, the EPR saturation behavior of cytochrome *a* was compared to that of cytochrome *c* and metmyoglobin-azide. The effects on the EPR saturation and lineshape of the Cu_A signal of changing the spin- and redox-state of the cytochrome a_3-Cu_B site and of partially reducing cytochrome *a* were also examined. The data suggest the existence of a magnetic dipolar interaction between Cu_A and cytochrome *a*. The results have been used to estimate the distance between these sites.

MATERIALS AND METHODS

Sample Preparation—Beef heart cytochrome *c* oxidase was isolated by the procedure of Hartzell and Beinert (8). The purified protein was dissolved in 50 mM Tris/acetate buffer or 50 mM phosphate buffer, 0.5% Tween 20, pH 7.4, and stored at −85 °C until use. The preparations used in this work contained 7–9 nmol of heme a/mg of protein and the concentration was 0.20–0.25 mM aa_3.

Partially reduced, CO-associated cytochrome oxidase was prepared by degassing the samples by 4–5 cycles of evacuation and flushing with argon followed by the addition of CO (1 atm), phenazine methosulfate (2 μM), and the appropriate number of equivalents of NADH. 0.01 equivalent (~2 μM) cytochrome *c* was included in these samples to ensure redox equilibrium; the EPR spectrum of cytochrome *c* (g = 3.06, 2.24, and 1.24) is not expected to interfere with the EPR spectrum of Cu_A in the region of interest (g = 1.95–2.15). Samples were incubated for 90 min at 4 °C to allow redox equilibration, and the extent of reduction was verified by optical absorption measurements in the 700–500 nm region. Fully reduced samples showed negligible (<1%) signals from adventitious copper.

French bean plastocyanin, *Pseudomonas aeruginosa* azurin, *Rhus vernicifera* stellacyanin, and *Rhus vernicifera* laccase were the generous gift of Professor Harry B. Gray of the Department of Chemistry, California Institute of Technology. The protein concentrations were 0.5, 0.5, 0.5, and 0.2 mM, respectively.

Bis(*N*-*t*-butylsalicylaldiminato) Cu(II) was synthesized by the method of Sacconi and Ciampolini (9) and was recrystallized from cyclohexane twice before use. The sample used to record the EPR

* This paper is Contribution 6823 from the Arthur Amos Noyes Laboratory of Chemical Physics, California Institute of Technology, Pasadena, CA 91125. The costs of publication of this article were defrayed in part by the payment of page charges. This article must therefore be hereby marked "*advertisement*" in accordance with 18 U.S.C. Section 1734 solely to indicate this fact.

‡ Recipient of National Research Service Award 5T32GM-07616 from the National Institute of General Medical Sciences. Present address, Department of Chemistry, Yale University, New Haven, CN 06520.

§ Recipient of National Research Service Award 5T32GM-07616 from the National Institute of General Medical Science.

¶ Recipient of Grant GM-22432 from the National Institute of General Medical Sciences and Biomedical Research Support Grant RR 07003. To whom reprint requests should be sent.

TABLE I

Temperature dependence of $(T_1T_2)^{-1}$

Species	Temperature dependence[a]
Plastocyanin	4.2
Azurin	3.9
Stellacyanin	4.2
Average of type 1 coppers	4.1
Laccase type 2	3.4
bis(*N*-*t*-butylsalicylaldiminato)Cu(II)	3.2
Cu(II)-EDTA 1	3.7
Cu(II)-EDTA 2	3.2
Average of inorganic coppers	3.4
Cysteine-HCl (g_z = 2.29)	5.1
Cysteine-HCl (g_z = 2.06)	3.6
Cysteine in glass (g_z = 2.06)	4.1
Cu_A (native and cyanide derivative)	5.9
Cytochrome *c*	6.5 ($T > 12$ K)
Metmyoglobin-N_3^-	4.8 ($T > 12$ K)
Cytochrome *a* (native)	6.3 ($T > 12$ K)
Cytochrome *a* (cyanide derivative)	4.3 ($T > 12$ K)

[a] Based on linear least squares fit of the data to: $-\log T_1T_2 = A \log T + B$. The temperature dependence is contained in the coefficient A.

spectra was dissolved in anhydrous methanol to a concentration of 0.8 mM. Cu(II)-EDTA was prepared by the addition of $CuCl_2$ to a 0.1 M solution of EDTA, pH 7.4, to give a final copper concentration of 1 mM.

The sulfur radicals were prepared by UV irradiation of cysteine. The two types of samples used were (i) polycrystalline cysteine-HCl and (ii) a saturated solution of cysteine-HCl in a 2:1 mixture of ethylene glycol/H_2O (the frozen solution formed a glass). Both types of samples were placed under an Ar atmosphere and irradiated at 77 K with a 200-watt Hg-Xe arc lamp. EPR spectra were recorded without warming the samples. A variety of sulfur radicals are formed by the UV irradiation (10, 11). These radicals exhibit a range of *g*-anisotropy and the g_{max} components of the EPR spectra of two separate sulfur radicals were resolved well enough to permit measurement of the EPR saturation of each radical independently.

All EPR spectra were recorded on anaerobic samples. The samples were made anaerobic by three cycles of evacuation and flushing with argon and, thereafter, were stored under an atmosphere of argon.

EPR Spectroscopy—The EPR spectra were recorded in the absorption mode on a Varian E-line century series X-band spectrometer employing 100 kHz field modulation. Incident microwave power was read on the E-109 leveled attenuator scale and was calibrated by measurement of both a nonsaturating Varian "strong pitch" sample and solid DPPH[1] at room temperature. Temperature regulation was achieved with an Air Products Heli-Trans low temperature system. The temperature was measured immediately before and immediately after recording the EPR spectra with a calibrated Au(0.07% Fe)-chromel thermocouple which was placed in an oil-filled EPR tube. The temperature was found to be stable to within 0.5 K for all the spectral measurements.

The samples were contained in 5-mm outer diameter (3.4-mm inner diameter) quartz EPR tubes. In most cases sufficient sample was placed in the EPR tubes to fill completely the TE 102 microwave cavity (only for the *Rhus* laccase sample was the amount insufficient to fill the cavity). Correction for the distribution of the microwave magnetic field, H_1, within the sample was neglected.

Data Analysis—For all of the complexes examined, the EPR line widths were largely determined by inhomogeneous broadening, at least at the lower temperatures studied. Inhomogeneous broadening arises from a number of mechanisms including unresolved hyperfine and dipolar interactions, *g*-anisotropy, "*g*-strain," etc. For proteins, *g*-strain is usually the largest contribution to the inhomogeneous line width. Castner (12) has shown that when an inhomogeneously broadened resonance is observed with incident microwave power, *P*, the EPR absorption amplitude, *Y*, is given by

$$Y = \frac{Y_0P^{1/2}}{(1 + \alpha P)^{1/2}} \exp(a^2\alpha P) \left\{\frac{1 - \phi[a(1 + \alpha P)^{1/2}]}{1 + \phi(a)}\right\} \quad (1)$$

where $\phi(x)$ is the error function

$$\phi(x) = \frac{2}{\sqrt{\pi}} \int_0^x \exp(-u^2)du, \quad (2)$$

Y_0 is a constant proportional to the number of spins in the resonant field, α is a saturation parameter proportional to the product of T_1 and T_2, and a is the ratio of the homogeneous line width and the inhomogeneous line width and hence a parameter which measures the degree of inhomogeneous broadening. Equation 1 can be reduced in the limit where $a = 0$ (inhomogeneous limit) and where $a \gg 1$ (homogeneous limit).

$$a = 0 \qquad Y = \frac{Y_0P^{1/2}}{(1 + \alpha P)^{1/2}} \quad (3)$$

$$a \gg 1 \qquad Y = \frac{Y_0P^{1/2}}{(1 + \alpha P)} \quad (4)$$

For situations intermediate between the inhomogeneous and homogeneous limits, the EPR absorption amplitude can be fitted empirically (13, 14) to the function

$$Y = \frac{Y_0P^{1/2}}{(1 + \alpha P)^{b/2}} \quad (5)$$

where b is the "inhomogeneity parameter" and may vary from 1.0 in the inhomogeneous to 2.0 in the homogeneous limit. A similar equation holds for the EPR absorption derivative amplitude (the quantity measured in this work), except that b may vary between 1.0 (inhomogeneous limit) and 4.0 (homogeneous limit).

The EPR saturation data in this work were fitted to Equation 5 by a nonlinear least squares routine. Initially, Y_0, α, and b were allowed to vary simultaneously. For a given paramagnetic compound, b is expected to increase monotonically with temperature from b ($T \to 0$) $\approx$ 1.0 to b (high T) $\approx$ 4.0. This is because the homogeneous line width $\left(\Delta H_2 = \frac{1}{\gamma T_2}\right)$ becomes small at low temperature as T_2 becomes long, and large at high temperature when T_2 becomes short, whereas the inhomogeneous line width remains constant. A second least squares fit of the saturation data to Equation 5 was performed in which only Y_0 and α were allowed to vary; in each case b was specified to ensure that b varied smoothly with temperature for each sample. The values of b were chosen on the basis of the initial least squares fit. Since the line width of the Cu_A signal was found to be very nearly constant within the temperature range studied, b was set equal to 1 (inhomogeneous limit) in the experiment comparing the saturation behavior of the Cu_A signal in the oxidized and partially reduced CO derivatives of the enzyme. In all cases, a satisfactory fit to the data was obtained by this procedure.

The product of T_1 and T_2 was obtained from the parameter α by the use of DPPH as a standard. At room temperature, $T_1 = T_2 = 2 \times 10^{-8}$ s for solid DPPH (15). On this basis, the proportionality between T_1T_2 and α was determined to be

$$T_1T_2 = 2.1\alpha \qquad (\text{in } \mu s^2). \quad (6)$$

An independent measurement of T_1 and T_2 for bis(*N*-*t*-butylsalicylaldiminato) Cu(II) by pulsed methods yielded a comparable proportionality between T_1T_2 and α (in this case it was found that $T_1T_2 = 8.2\alpha$).

RESULTS

Comparison of the EPR Saturation Data—The EPR saturation for several type 1 copper proteins, the type 2 copper in laccase (for a review of type 1 and type 2 copper proteins, see Ref. 16), several inorganic Cu(II) complexes, several sulfur radicals, several low spin heme proteins, and the Cu_A center in both the native and in partially reduced CO complexes of cytochrome oxidase was examined over a range of temperatures (Figs. 1–6). We first will discuss the relaxation differ-

[1] The abbreviation used is: DPPH, α,α'-diphenyl β-picrylhydrazyl.

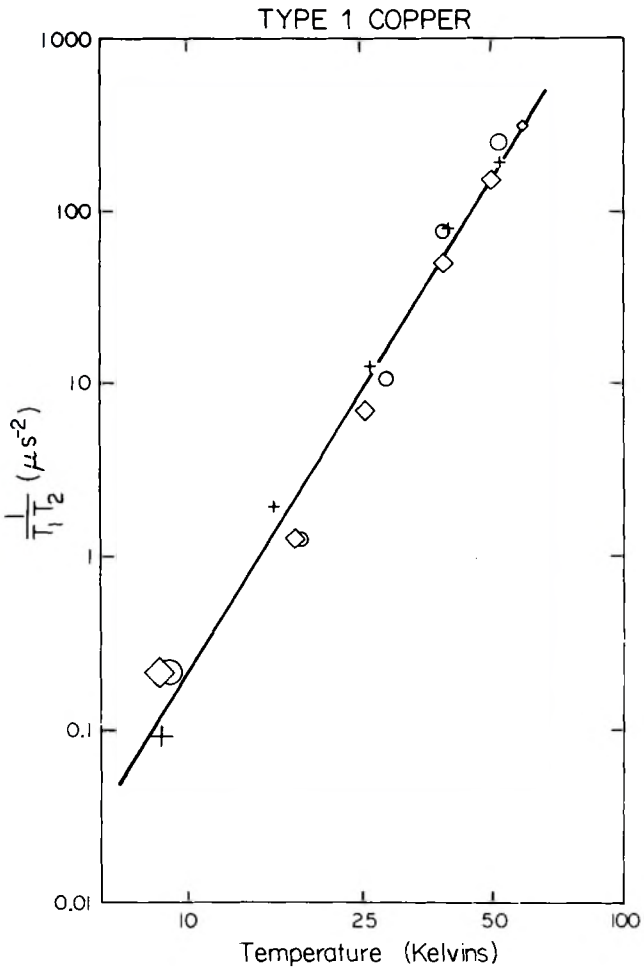

FIG. 1. **EPR relaxation of type 1 coppers.** The *size* of the *points* reflects the estimated error in T and $(T_1T_2)^{-1}$. *Circles* denote stellacyanin; *diamonds* denote azurin; and *crosses* denote plastocyanin. The EPR saturation was measured by the peak height of the EPR signal at g_y in all cases.

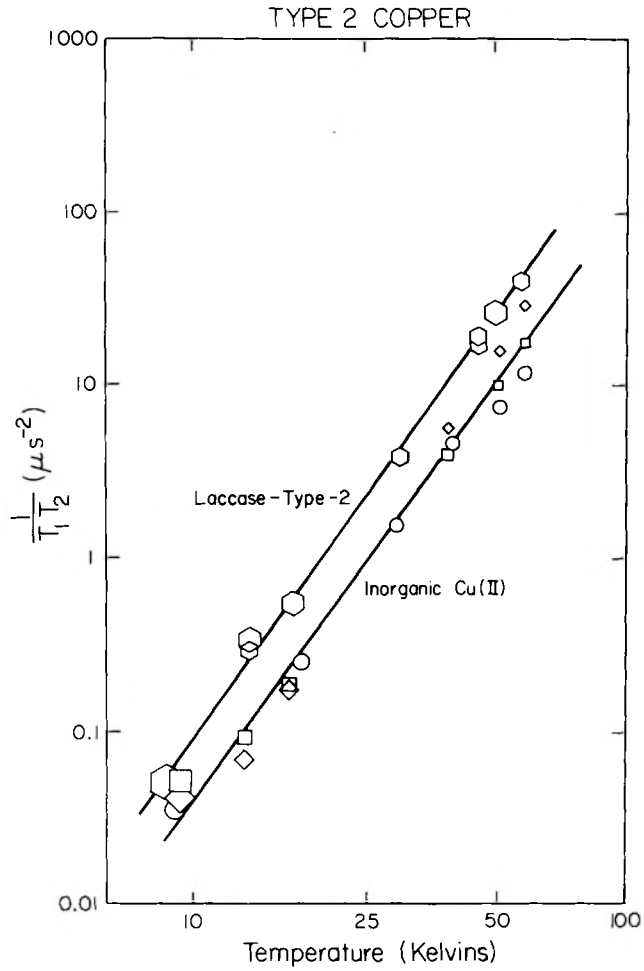

FIG. 2. **EPR relaxation of the type 2 copper in laccase and the inorganic Cu(II) complexes.** The *size* of the *points* reflects the estimated error in T and $(T_1T_2)^{-1}$. *Hexagons* denote the type 2 copper in laccase; *diamonds* denote Cu-EDTA 1; *squares* denote Cu-EDTA 2; and *circles* denote bis(*N*-*t*-butylsalicylaldiminato) Cu. Cu-EDTA 1 had $g_{11} = 2.32$ and $A_{\parallel} = 0.0147$ cm^{-1}, while Cu-EDTA 2 had $g_{\parallel} = 2.28$ and $A_{\parallel} = 0.0160$ cm^{-1}. The difference in these two complexes probably was due to the protonation of two of the carboxyl groups of EDTA in Cu-EDTA 1 and only one of the carboxyl groups in Cu-EDTA 2. The EPR saturation was measured by the peak height of the EPR signal at g_{max} for all the above complexes except bis(*N*-*t*-butylsalicylaldiminato) Cu, which was monitored at g_y.

ences noted among the various samples.

Each of the species for which EPR saturation was measured has associated with it an unpaired electron spin of ½. However, the magnitude of the *g*-anisotropy varies considerably among the samples. In Fig. 7 we have plotted log T_1T_2 observed at 10, 20, and 40 K *versus* the *g*-anisotropy of the paramagnetic species. We note that for cysteine radicals, type 2 Cu(II), inorganic Cu(II), and low spin ferrihemes, there is a nearly linear relation between log (T_1T_2) and the *g*-anisotropy and that the proportionality relating the two quantities is constant over the temperature range $20 \leq T \leq 40$ K (note the parallel slopes in Fig. 7, *center* and *right* panels), although at 10 K the dependence of log (T_1T_2) on the *g*-anisotropy is considerably weaker. In any case, the observed proportionality between log (T_1T_2) and the *g*-anisotropy indicates that the spin-lattice relaxation is dominated by the Van Vleck mechanism (for a discussion of spin-lattice relaxation, see Ref. 17) for these compounds. The weaker dependence of log(T_1T_2) on *g*-anisotropy at 10 K merely reflects the increasing importance of the direct process at the lower temperature. The Raman process clearly dominates at temperatures above 20 K.

Although the type 1 coppers and the Cu_A center both show relaxation rates greater than expected on the basis of their *g*-anisotropy, there is an important difference between the temperature dependences of their relaxation behavior. The T_1T_2 product for the type 1 coppers is about 6–7 times shorter than that of the other species with comparable *g*-anisotropy at *all* the temperatures examined. The relaxation of the Cu_A center is actually close to that expected on the basis of the *g*-anisotropy at 10 K, but as the temperature is increased, the relaxation of the Cu_A center becomes increasingly faster than that of the other species.

The temperature dependence of the T_1T_2 product for all of the complexes examined is given in Table I. We find that in all cases the average temperature dependence of $(T_1T_2)^{-1}$ varies between T^3 and T^7 over the temperature range 12 to 50 K, with a tendency towards a somewhat weaker temperature dependence with increasing temperature in most cases. These observations are consistent with the temperature dependence expected if the spin-lattice relaxation is dominated by the Van Vleck Raman mechanism; however, for the protein species which exhibit relatively weak temperature dependence ($T^{<5}$) it is likely that the Debye temperature is in this range. Otherwise, the fractal dimension of these proteins would be smaller than appears possible (<1) (*vide infra*).

The Cu_A Center in Cytochrome c Oxidase—On the basis of

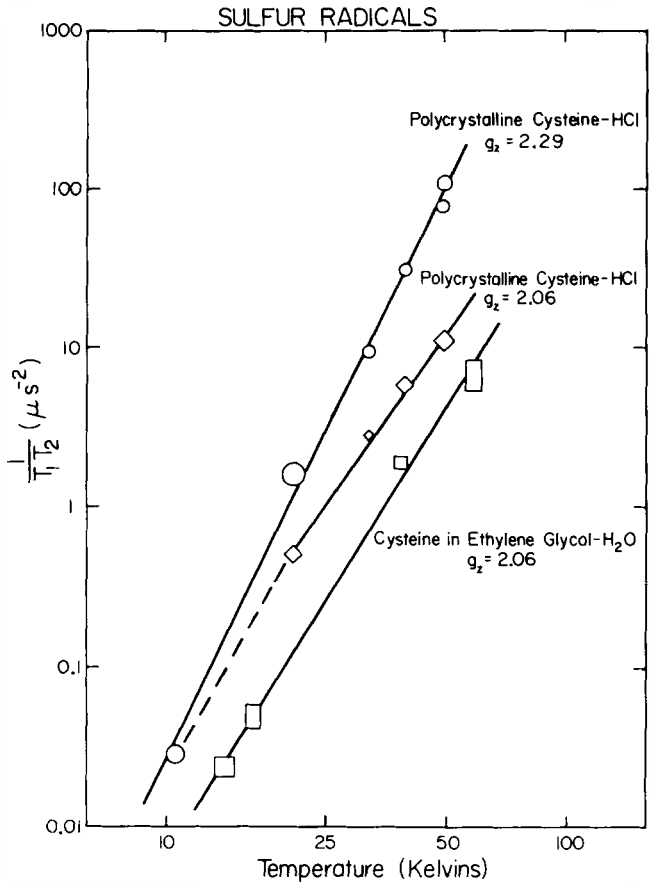

FIG. 3. **EPR relaxation of sulfur radicals.** The *size* of the *points* reflects the estimated error in T and $(T_1T_2)^{-1}$. The EPR saturation was measured by the peak height of the EPR signal at g_{max} in all cases.

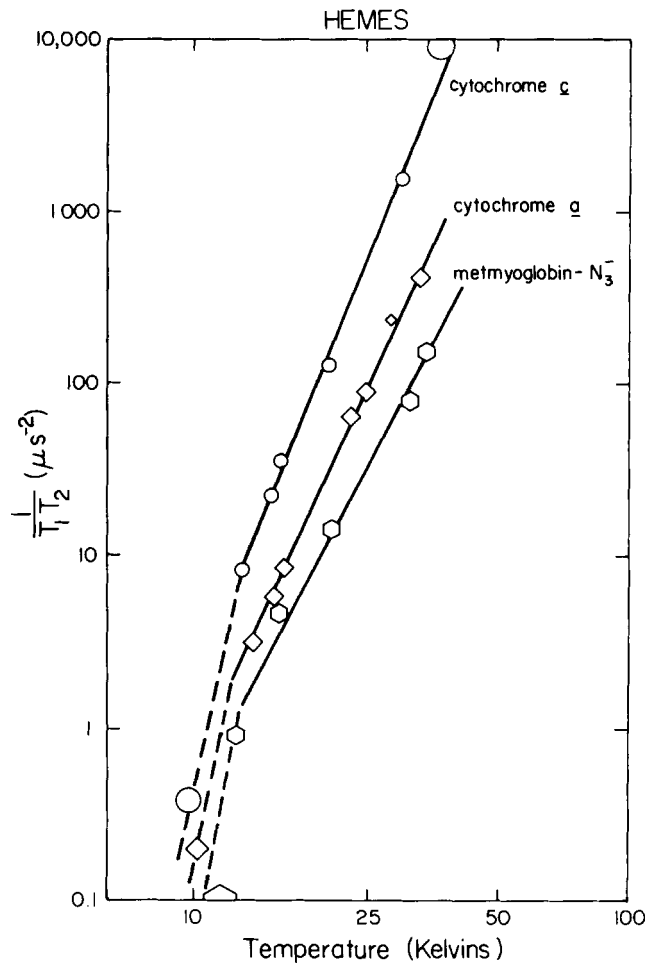

FIG. 4. **EPR relaxation of low spin hemes.** The *size* of the *points* reflects the estimated error in T and $(T_1T_2)^{-1}$. The *dotted lines* drawn below 12 K are to emphasize that the temperature dependence of the low spin hemes has a break at about 12 K. The EPR saturation was measured by the peak height of the EPR signal at g_{max}.

our proposal that the Cu_A center is best described as a Cu(I)-sulfur radical complex (2, 3), the electron spin relaxation of the Cu_A center might be expected to be similar to that of a sulfur radical or possibly intermediate between a sulfur radical and a Cu(II) ion. For this comparison, the cysteine sulfur radical with g-values of 2.29, 1.99, and 1.99 would be the most appropriate. In fact, below 10 K the spin relaxation of the Cu_A center is indeed very similar to that of this cysteine sulfur radical. However, as can be seen from Fig. 5, the T_1T_2 behavior of the Cu_A center is overall quite different from that of the sulfur radicals or any of the Cu(II) compounds examined, including the type 1 coppers. In particular, at temperatures above 20 K, the Cu_A center shows a much more rapid electron spin relaxation than any of the sulfur radicals or Cu(II) compounds examined. These observations suggest that the environment of the Cu_A site is unlike that of any of the other copper complexes studied, and/or that the spin relaxation of the Cu_A center is influenced by its proximity to one or more of the other metal centers in the protein. Cytochrome *a* has a significantly faster relaxation rate than the Cu_A center (Figs. 4 and 5). The cytochrome a_3-Cu_B site, being $S = 2$, is also expected to have a faster relaxation rate than any of the $S = ½$ species examined in this work. Thus, if the more slowly relaxing Cu_A center were close to either one of the hemes, then the heme(s) would be expected to increase the relaxation rate of the Cu_A center substantially (18), particularly at higher temperatures.

It is possible to ascertain whether or not the Cu_A center is close to the cytochrome a_3-Cu_B site by examining the effect of partial reduction and CO binding on the spin relaxation of the Cu_A center. In the oxidized enzyme, cytochrome a_3 and Cu_B together form an $S = 2$ site (19). However, when these metals are reduced in the presence of CO, the site becomes diamagnetic since the cytochrome a_3-CO complex is expected to be low spin. The spin relaxation of the Cu_A center is not significantly affected by the formation of this partially reduced CO complex (Fig. 6). The lineshape of the Cu_A signal does not show significant changes either (caption to Fig. 8). When the enzyme is further (~1 additional electron equivalent) reduced, a significant effect, corresponding to a 50% increase in T_1T_2, is observed. In this sample, cytochrome *a* is ~75% reduced and Cu_A is ~35% reduced. Assuming that the reduction potentials of these sites are not positively correlated (we have observed no cooperativity of this kind in redox titrations of cytochrome *a* and Cu_A), this means that at least 75% of the observed Cu_A signal originates from cytochrome oxidase molecules in which cytochrome *a* is reduced and therefore diamagnetic. The substantial change in T_1T_2 of the Cu_A signal in this experiment thus suggests that the relaxation of Cu_A is influenced by a dipolar interaction with cytochrome *a*.

A small lineshape change ($\Delta g_y \cong 0.001$) in the Cu_A signal upon cytochrome *a* reduction was also observed in these experiments (Fig. 8). This change persisted at a high temperature (62 K, data not shown) where a dipolar splitting of moderate strength due to cytochrome *a* is expected to be

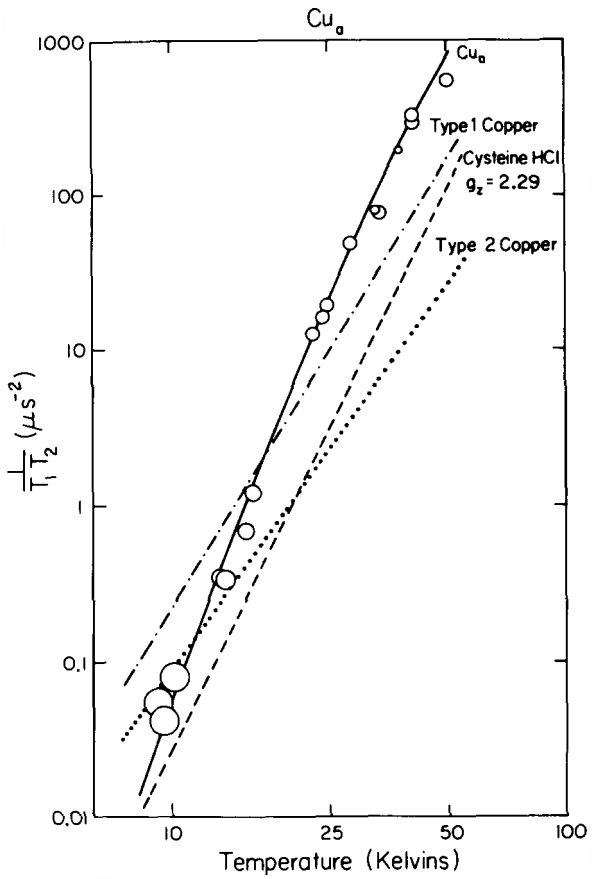

FIG. 5. **EPR relaxation of the Cu_A center in cytochrome *c* oxidase.** The *size* of the *points* reflects the estimated error in T and $(T_1T_2)^{-1}$. For comparison, the *lines* drawn through the type 1 copper, cysteine-HCl (g_z = 2.29), and the type 2 copper in laccase data from Figs. 3–5 are shown. The EPR saturation was measured by the peak height of the EPR signal at g_y.

largely relaxed, so it is likely that the Cu_A site undergoes a small structural change in response to the reduction of cytochrome *a*.

Cytochrome a—The EPR saturation of cytochrome *a* is typical of that expected for a low spin heme with *g*-values of 3.00, 2.24, and 1.49. Both the magnitude of T_1T_2 (Fig. 7) and its temperature dependence (Fig. 4) are in agreement with the values predicted by comparison with other low spin ferrihemes. The EPR saturation properties of cytochrome *a* therefore indicate that T_1 and T_2 of cytochrome *a* are not significantly affected by any of the other metal centers in cytochrome *c* oxidase.

DISCUSSION

Mechanism of Spin Relaxation—The temperature dependence and the magnitude of T_1T_2 for all of the complexes examined can be reasonably accounted for if the Van Vleck Raman process dominates the spin-lattice relaxation (see Fig. 7 and Table I). It was previously concluded that the Van Vleck Raman process determines the spin-lattice relaxation for organosulfur radicals (10) and also for cytochrome *c* (20, 21). Our measurements extend these observations to include type 1 copper, type 2 copper, Cu_A in cytochrome *c* oxidase, inorganic Cu(II) coordinated to oxygen and nitrogen ligands, and several low spin ferrihemes including cytochrome *a* in cytochrome oxidase. Earlier we pointed out that the product T_1T_2 for type 1 copper was about 6–7 times shorter than that of several other species with comparable *g*-anisotropy

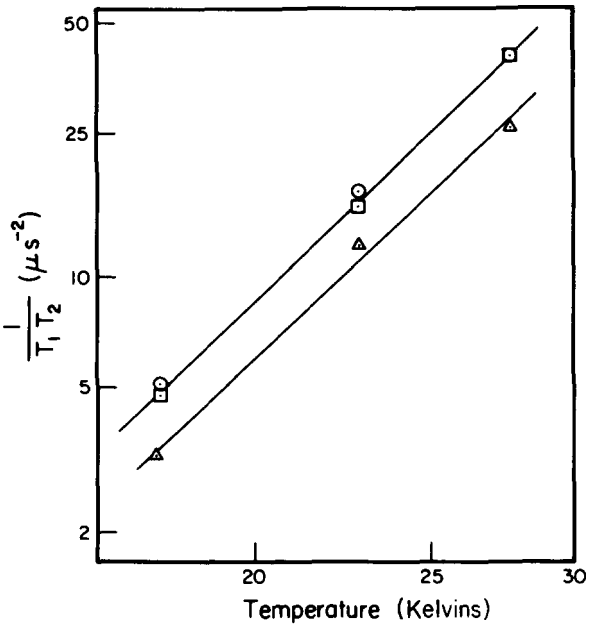

FIG. 6. **EPR relaxation of the Cu_A center in native oxidized and partially reduced CO complexes of cytochrome *c* oxidase.** *Circles* denote the native oxidized enzyme to which 1 atm of CO was added followed by freezing (no reduction of the Fe_{a_3}/Cu_B site was detected by optical measurements of this sample). *Squares* denote the ~2-electron reduced CO complex; *triangles* denote the ~3.0-electron reduced CO complex. Details of sample preparation are given under "Materials and Methods." The EPR spectra were measured at g_y.

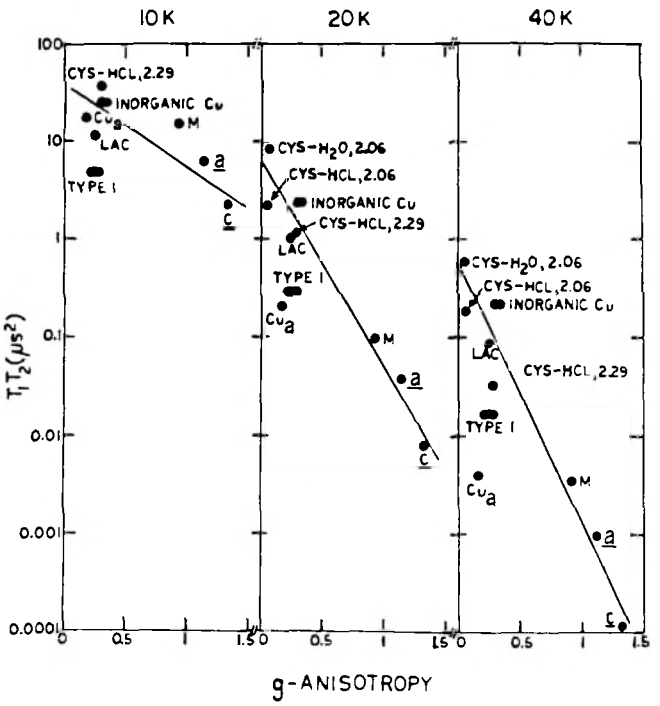

FIG. 7. **EPR relaxation *versus* the *g*-anisotropy for all of the complexes studied at 10, 20, and 40 K.** The *g*-anisotropy was taken to be $[(g_x - 2)^2 + (g_y - 2)^2 + (g_z - 2)^2]^{1/2}$. *Lac*, laccase type 2 copper; *cys-H_2O, 2.06*, cysteine sulfur radical in ethylene glycol/H_2O with g_z = 2.06; *cys-HCl, 2.06*, cysteine sulfur radical in polycrystalline cysteine-HCl with g_z = 2.06; *cys-HCl, 2.29*, cysteine sulfur radical in polycrystalline cysteine-HCl with g_z = 2.29; *M*, metmyoglobin-azide; *a*, cytochrome *a*; *c*, cytochrome *c*.

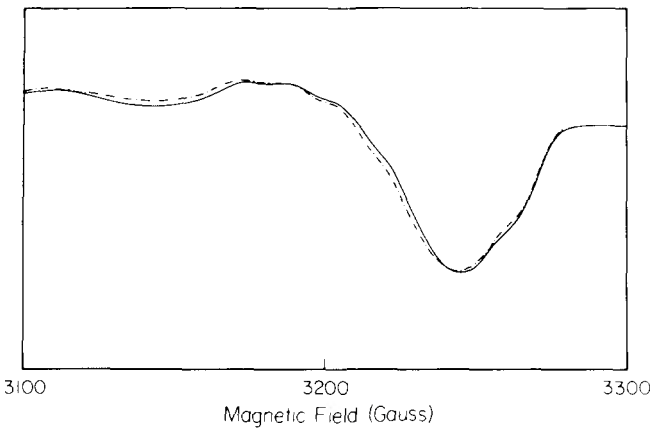

FIG. 8. **Expanded EPR spectra of Cu_A in the $g = 1.95–2.10$ region in 2-electron reduced CO-associated (*solid line*) and ~3-electron reduced CO-associated (*dashed line*) cytochrome *c* oxidase.** The EPR spectrum of the resting oxidized enzyme was not significantly different from that of the 2-electron reduced CO-associated enzyme, so for the sake of clarity it is omitted. Conditions of EPR spectroscopy: Microwave frequency = 9.172 GHz; modulation frequency = 100 kHz; modulation amplitude = 6.3 G, microwave power = 0.2 milliwatt, temperature = 14 K.

throughout the temperature range studied (10–50 K). This suggests the possibility of an alternate relaxation pathway here. We find that the temperature dependence of T_1T_2 for the type 1 coppers could not be accounted for well by assuming that the spin-lattice relaxation is dominated by an Orbach process (22). In light of this, we must conclude that the spin-lattice relaxation of the type 1 coppers also proceeds via the Van Vleck Raman mechanism and that the coupling of the phonon bath to the spin center is more effective in the case of type 1 copper than for the other Cu(II) complexes examined. The coupling of the phonon bath to the spin center depends on a number of variables. Most important is the lattice structure about the spin center. In this regard, it is interesting that the cysteine sulfur radical with $g_z = 2.06$ shows a significantly slower relaxation rate in an ethylene glycol-H_2O matrix than in crystalline cysteine-HCl (Fig. 3).

The relaxation rate of Cu_A exhibits a stronger temperature dependence than that of any of the other copper species examined. This unusual temperature dependence is the same in the fully oxidized and partially reduced cytochrome oxidase species (Fig. 6), which indicates that it does not arise from a magnetic dipolar interaction between Cu_A and cytochrome *a*. A recently elaborated theory of spin relaxation in metalloproteins has demonstrated that the temperature dependence of relaxation rates in these systems will correlate with the fractal dimension of the protein surrounding the spin center, specifically that a greater fractal dimension (tighter protein folding) will lead to a steeper temperature dependence. This means that the protein in the environment of Cu_A is more tightly folded than that surrounding the type 1 or 2 copper centers studied in this work. The solvent, which effectively has a low fractal dimension, will constitute a larger fraction of the environment of a site which is relatively solvent-exposed, so our observation may alternatively be taken as evidence that Cu_A is more deeply buried in the protein than are the type 1 or type 2 coppers. The close similarity of the temperature dependences in the 2- and 3-electron reduced species indicates that the overall protein folding near Cu_A, and the degree of exposure of this site to the solvent, are not measurably affected by the reduction of cytochrome *a*.

A small, temperature-independent shift in one of the Cu_A *g*-values ($\Delta g \approx 0.001$) (Fig. 8) occurs upon cytochrome *a* reduction, which signals a minor structural change at the Cu_A site. In view of the smallness of the spectral change and the similar relaxation rate-temperature dependences in the two species, however, it is unlikely that the structural change involved is responsible for the observed difference in absolute relaxation rates in the 2- and 3-electron reduced species. Apart from the small shift in g_y, the Cu_A lineshapes are very similar in the 2- and 3-electron reduced species. The temperature dependences between 20 and 62 K of the lineshapes in the $g = 1.95–2.15$ region (not shown) are also very similar. A dipolar interaction of moderate strength (10–25 G), which would have been manifested at the low end of this temperature range, would be largely collapsed at the high end (*vide infra*). We note that a wide range of molecular orientations was sampled in this experiment as a large portion of the spectrum was studied. Since only a fraction of these orientations can correspond to those for which a dipolar interaction is unfavorable (*i.e.* those close to the magic angle), we conclude that substantial (>10 G) magnetic dipolar splittings due to cytochrome *a* are not contributing to the Cu_A lineshape. This absence of >10 G splittings indicates a distance between cytochrome *a* and Cu_A which is in excess of 13 Å (*vide infra*).

A comparison of the saturation of the Cu_A signal in the native and in partially reduced CO derivatives of the enzyme furnishes evidence for a magnetic dipolar interaction between Cu_A and cytochrome *a* which influences the relaxation of Cu_A. It is important to note that the dipolar contribution to $1/T_1$ adds to the intrinsic rate $1/T_1^0$. The contribution of the dipolar mechanism of relaxation to the total relaxation rate will only be significant if the intrinsic relaxation rate is less than, or approximately equal to, the dipolar relaxation rate. Hence, a rapidly relaxing site can strongly effect the relaxation of a nearby slowly relaxing site, while the reverse interaction is insignificant compared to the intrinsic relaxation rate of the rapidly relaxing site. We believe that such is the case for the interaction between cytochrome *a* (rapid intrinsic relaxation) and the Cu_A center (slow intrinsic relaxation).

A significant magnetic interaction between Cu_A and the Fe_{a_3}/Cu_B site was not observed, in spite of the fact that this site has a greater spin ($S = 2$) and is expected to relax faster than cytochrome *a*. However, these observations are not readily interpreted in terms of an intersite distance for the following reasons. The magnetic moment of the Fe_{a_3}/Cu_B site is oriented chiefly by the zero field splitting of the heme, which is expected to be on the order of 10 cm^{-1}, rather than by the applied magnetic field. The Fe_{a_3}/Cu_B magnetic moment is quantized roughly along the heme normal, and its static component will be small in the $m_s = 0$ ground state expected in this antiferromagnetically coupled system (m_s is the component of the spin angular momentum along the axis of quantization). Higher lying (by ~10–20 cm^{-1}) states with $m_s = \pm1, \pm2$ will be ~30 and ~10% populated, respectively, at the lower end of the temperature range examined; only these will have significant static magnetic moments. Static dipolar splittings of the Cu_A signal by the Fe_{a_3}/Cu_B spin system will therefore not necessarily be large, in spite of the larger overall spin of the system. One other factor will also act to minimize dipolar splittings, *i.e.* rapid spin-lattice relaxation of the Fe_{a_3}/Cu_B spin system will collapse such splittings (*vide infra*), particularly at higher temperatures.

Similar considerations apply to the enhancement of Cu_A spin relaxation by the Fe_{a_3}/Cu_B spin system. One mechanism of relaxation enhancement involves principally the static component of the Fe_{a_3}/Cu_B magnetic moment (*cf.* Equations 8 and 10 below), which, as noted above, may be small. Also, in this mechanism, extremely rapid spin-lattice relaxation of

the fast-relaxing spin system will lead to less efficient enhancement of the relaxation of the slow-relaxing spin. Another mechanism of relaxation enhancement (*cf.* Equation 7 below) involves chiefly the precessing component of the Fe_{a_3}/Cu_B magnetic moment, which in an $S = 2$ system will precess too quickly to be effective in relaxing the much more slowly precessing spin of Cu_A.

Disposition of the Metal Centers of Cytochrome c Oxidase—Since the structural change at Cu_A due to the reduction of cytochrome *a* is apparently very small, it is most likely that the observed effect on the spin relaxation of Cu_A is due to a magnetic dipolar interaction between Fe_a and Cu_A. On the basis of this assumption, we may use the relaxation data to place limits on the distance between cytochrome *a* and Cu_A.

The product T_1T_2 is the quantity which is measured in our experiments and in similar experiments from other laboratories (20, 23). We must therefore consider two equations describing the dipolar-induced relaxation, one for the change in T_1 and one for the change in T_2. For the case of weak interactions, which will be defined below, these are (18)

$$\frac{1}{T_{1s}} = \frac{1}{T_{1s}^0} + J(J+1) \cdot \left[\frac{b^2 T_{2f}}{1+(\omega_f-\omega_s)^2T_{2f}^2} + \frac{c^2T_{1f}}{1+\omega_s^2T_{1f}^2} + \frac{e^2T_{2f}}{1+(\omega_f+\omega_s)^2T_{2f}^2}\right] \quad (7)$$

and

$$\frac{1}{T_{2s}} = \frac{1}{T_{2s}^0} + J(J+1)\left[A^2T_{1f} + \frac{B^2T_{2f}}{1+\omega_f^2T_{2f}^2} + \frac{C^2T_{2f}}{1+(\omega_f-\omega_s)^2T_{2f}^2} + \frac{D^2T_{1f}}{1+\omega_s^2T_{1f}^2} + \frac{E^2T_{2f}}{1+(\omega_f+\omega_s)^2T_{2f}^2}\right] \quad (8)$$

where

$$b^2 = \frac{1}{6}\gamma_f^2\gamma_s^2\hbar^2r^{-6}(1-3\cos^2\theta)^2$$

$$c^2 = \frac{3}{4}\gamma_f^2\gamma_s^2\hbar^2r^{-6}\sin^2 2\theta$$

$$e^2 = \frac{3}{2}\gamma_f^2\gamma_s^2\hbar^2r^{-6}\sin^4\theta$$

$$A^2 = \frac{1}{3}\gamma_f^2\gamma_s^2\hbar^2r^{-6}(1-3\cos^2\theta)^2$$

$$B^2 = \frac{3}{4}\gamma_f^2\gamma_s^2\hbar^2r^{-6}\sin^2 2\theta$$

$$C^2 = \frac{1}{12}\gamma_f^2\gamma_s^2\hbar^2r^{-6}(1-3\cos^2\theta)^2$$

$$D^2 = \frac{3}{8}\gamma_f^2\gamma_s^2\hbar^2r^{-6}\sin^2 2\theta$$

and

$$E^2 = \frac{3}{4}\gamma_f^2\gamma_s^2\hbar^2r^{-6}\sin^4\theta$$

The indices *s* and *f* refer to the slow-relaxing and fast-relaxing spins, respectively; r is the intersite distance; θ is the angle between the intersite vector and the applied magnetic field; γ is the magnetogyric ratio; and ω is the precession frequency in the applied field.

These equations are only valid under conditions where first order time-dependent perturbation theory is applicable. In the case of Equation 8, this condition is equivalent to

$$\frac{\vec{\mu}_f\cdot\vec{\mu}_s}{r^3} < \frac{\hbar}{T_{1f}} \quad (9)$$

where the μs are magnetic moments. This condition is most easily satisfied at higher temperature; at the highest temperature studied (28 K), it would require a site separation greater than or equal to approximately 30 Å (T_1 for cytochrome *a* at 28 K is estimated below). This is larger than expected and, as we shall see, larger than is necessary to explain the observed effect.

In the opposite, namely strong interaction limit, the appropriate analogue of Equation 8 is

$$\frac{1}{T_{2s}} = \frac{1}{T_{2s}^0} + \frac{1}{2T_{1f}} \quad (10)$$

This equation implies that each time the fast-relaxing spin undergoes longitudinal relaxation the slow-relaxing spin undergoes complete transverse relaxation. Equation 10 does not contain r, so distance estimates may not be obtained from it directly. In the strong interaction limit, however, Cu_A will "see" cytochrome *a* as a static magnetic dipole (24). This leads to splittings in the Cu_A spectrum which are related to intersite distance and orientation by $\Delta H = (g\beta(3\cos^2\theta - 1))/r^3$ where ΔH is the splitting in gauss. For $g = 2$ and $(3\cos^2\theta - 1) = 1$, a 13 Å separation will lead to an ~10 G splitting. Thus, the absence of moderate (~10 G) dipolar splittings due to cytochrome *a* in the Cu_A EPR spectrum indicates an intersite distance in excess of 13 Å, as was noted above.

In the case of Equation 7, the weak interaction condition is less restrictive, since it will involve an effective interaction time which is maximally $T_{2f}/((\omega_f - \omega_s)^2T_{2f}^2)$, which is much smaller than T_{1f}. Equation 7 is therefore valid at much shorter distances (≲10 Å), and we need not consider the strong interaction analogue of Equation 7.

In some previous treatments of the spin interaction problem (23), attention was directed to Equation 7, and Equation 8 or its strong interaction analogue was neglected completely on the assumption that

$$\frac{1}{T_{2s}} \gg \frac{1}{T_{1s}} \quad (11)$$

In such a situation, increments to $1/T_{2s}$ will have a much smaller effect on $1/T_{1s}T_{2s}$ than will increments to $1/T_{1s}$. As we shall see, this assumption is not always justified. Another important point to note is that the term containing b^2 in Equation 7 involves T_{2f}, not T_{1f} as assumed in previous treatments of spin interactions in cytochrome *c* oxidase (23, 25).

We may determine the relative importance of ΔT_1 and ΔT_2 effects by considering Equations 7 and 8 (or 10) separately. This is a useful way to begin the calculation because it will test the validity of the assumption that Equation 7 fully describes the dipolar-induced relaxation under our experimental conditions.

The application of Equations 7, 8, or 10 requires values for the relaxation times T_{1f}, T_{1s}, T_{2f}, and T_{2s}. Our measurements between 10 and 28 K enable us to specify the product T_1T_2, and recent measurements using a pulse saturation method (25) have yielded the values of T_{1f} and T_{1s} between 1.5 and 20 K. Using the T_1 values at ~20 K to scale our data and assuming that the temperature dependence between 20 and 28 K arises primarily from T_1, we obtain the following estimates (at 28 K):

$$\frac{1}{T_1}(a) \approx 4.2 \times 10^6\ s^{-1} \quad (12)$$

$$\frac{1}{T_2}(a) \approx 4.2 \times 10^7\ s^{-1} \quad (13)$$

$$\frac{1}{T_1}(\mathrm{A}) = 1.6 \times 10^6\ \mathrm{s}^{-1} \quad (14)$$

$$\frac{1}{T_2}(\mathrm{A}) = 2.3 \times 10^7\ \mathrm{s}^{-1} \quad (15)$$

Owing to our assumption that T_2 does not vary with temperature, these are upper limits on $\frac{1}{T_1}$ and lower limits on $\frac{1}{T_2}$.

Before applying Equation 7, we will make some simplifying approximations. These approximations do not weaken the important conclusions which we will draw from the calculations. The approximations are: 1) substitution of a spherically averaged value of 0.8 for the term $(3\cos^2\theta - 1)^2$; 2) setting $(\omega_f - \omega_s)$ equal to 6×10^9 rad·s^{-1} (we assume the *most probable* g-value for cytochrome a, *i.e.* 2.25); 3) using $J = \frac{1}{2}$ for cytochrome a and setting $\gamma_f = \gamma_s = \gamma_e$; and 4) retaining only the leading (b^2) term in Equation 7 (this term will be much larger than the other two, *cf.* Ref. 23). These approximations are not expected to lead to gross inaccuracies because a wide range of molecular orientations was probed in our experiment (the Cu_A signal intensity was measured at g_y). Since the cytochrome a signal is highly anisotropic, this means that a wide range of resonant frequencies of cytochrome a (ω_f) was sampled. Hence, it is not expected that $(\omega_f - \omega_s)$ is effectively much *less* than the above estimate; it can only be so for a restricted range of molecular orientations. Thus, our approximations tend to overestimate the intersite distance.

Under these assumptions, Equation 7 leads to $r = 5.4$ Å. This result is in clear contradiction to the lack of observable dipolar splittings at Cu_A due to cytochrome a. Apparently, the use of Equation 7 exclusively is not justified in the present case.

We may alternatively assume that only T_2 effects are important. Since $(1/T_1T_2)(\mathrm{A})$ is increased by ~50% due to the dipolar interaction with cytochrome a (Fig. 6) and $(1/T_2^0)(\mathrm{A}) \approx 1.53 \times 10^7\ \mathrm{s}^{-1}$, we have

$$\Delta\frac{1}{T_2}(\mathrm{A}) \approx 7.7 \times 10^6\ \mathrm{s}^{-1} \quad (16)$$

An upper limit on intersite distance may be obtained by noting that the precession frequency of Cu_A in the dipolar field of cytochrome a must be at least as large as $\Delta(1/T_2)(A)$. We thus have

$$7.7 \times 10^6 \leq \gamma_e H_d \quad (17)$$

where H_d is the dipolar field at Cu_A. If a spherically averaged value for the orientation parameter $(3\cos^2\theta - 1)$ is assumed, this gives $r \leq 26$ Å. We thus conclude that the distance between cytochrome a and Cu_A is between 13 and 26 Å. Also, it is apparent that in our experiments T_2 effects are dominant, in contrast to the assumptions of Ref. 23.

The above discussion pertains to the distance between Cu_A and cytochrome a. Recently, experiments have been performed (23, 25, 26) which address the question of the distance between the "a sites" (cytochrome a and Cu_A) and the cytochrome a_3/Cu_B site. In studies employing the nitrosyl adduct of ferrocytochrome a_3, estimates of the distance between $Fe^{2+}_{a_3}\cdot NO$ and either cytochrome a or Cu_A were obtained from dipolar splittings (26) or from relaxational effects (23, 25). The most detailed information regarding relaxation rates has come from the pulse saturation recovery experiments of Ref. 25, in which T_1s were measured directly. These experiments were analyzed according to Equation 7, but with T_{1f} incorrectly substituted for T_{2f} in the leading term. In the light of the above discussion, we have corrected these distance estimates by using a T_{2f} value estimated from the data above.

From our data (Figs. 4 and 5) and the 12 K data of Ref. 27, we find

$$\frac{1}{T_2}(\mathrm{A}) \approx \frac{1}{T_2}(a) \approx 1 \times 10^7\ \mathrm{s}^{-1}\ (\text{at } 12\ \mathrm{K}) \quad (18)$$

and

$$\frac{1}{T_1}(a) = 1.54 \times 10^5\ \mathrm{s}^{-1} \quad (19)$$

The correction to the $Fe^{2+}_{a_3}\cdot NO/Fe_a$ distance estimate in Ref. 25 is then just $(1 \times 10^7/1.54 \times 10^5)^{1/6}$ or a factor of 2.0. In Ref. 25, the maximum distance between nitrosylferrocytochrome a_3 and cytochrome a was estimated at 13 Å, so the corrected maximum distance estimate is 26 Å. If we again assume a typical relative orientation of the sites, rather than one which maximizes the interaction, we calculate an intersite distance of 20 Å. since $(1/T_2)(\mathrm{A})$ is not very different from $(1/T_2)(a)$, Cu_A is just as effective a relaxer of the $Fe^{2+}_{a_3}\cdot NO$ complex, via this mechanism, as is cytochrome a. In fact, since the g-values of Cu_A will lead to better resonance with the $Fe^{2+}_{a_3}\cdot NO$ spin for most molecular orientations, it is likely that Cu_A is a *better* relaxer than cytochrome a. One should therefore *not* conclude that cytochrome a is exclusively responsible for the dipolar enhancement of the $Fe^{2+}_{a_3}\cdot NO$ relaxation rate.

In Ref. 26, the distance between $Fe^{2+}_{a_3}\cdot NO$ and cytochrome a was estimated to be 15 Å on the basis of ~12 G static dipolar splittings of the $Fe^{2+}_{a_3}\cdot NO$ EPR signal. This estimate was based on the assumption that cytochrome a was responsible for the observed splittings and that Cu_A made no contribution. The observed splittings partially collapsed as the sample temperature was raised from 30 to 44 K; this has been taken as evidence that cytochrome a is the source of the splittings since at 44 K only cytochrome a is expected to relax quickly enough to substantially collapse a ~12 G splitting. However, the $Fe^{2+}_{a_3}\cdot NO$ signal continued to sharpen significantly between 54 and 77 K, which suggests a significant contribution to the dipolar splitting by the slower-relaxing Cu_A spin. Since both Fe_a and Cu_A are thus likely to contribute to the overall splitting, the 15 Å distance estimate between cytochrome a and cytochrome a_3 represents only a lower limit. Hence, these results are not inconsistent with the revised estimate of ~20 Å obtained above.

On the basis of our estimate of the distance between Cu_A and cytochrome a and the revised estimates of the a-site/a_3-site distances, we propose the metal center disposition illustrated in Fig. 9.

Implications of Intersite Distances for Electron Transfer Kinetics—Before concluding, it seems appropriate to comment upon the implications of the above distance estimates for intramolecular electron transfer rates. From stopped-flow and flow-flash kinetic studies (27–33), it is known that under

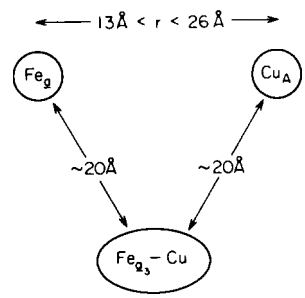

FIG. 9. **Proposed spatial distribution of the metal centers in cytochrome c oxidase.**

many conditions the rate-limiting step in the cytochrome oxidase reaction is intramolecular electron transfer. This fact is consistent with the considerable intersite distances which we are proposing. According to one theory (34), electron transfer over 20 Å in a saturated hydrocarbon environment is expected to have a rate on the order of only 1 s^{-1}, even if other factors influencing the rate are optimized. However, favorable alignment of the aromatic hemes and/or imidazole ligands to copper could enhance the rate substantially. The observed rates of electron transfer in cytochrome oxidase at room temperature are close to 1000 s^{-1}. If the above distance estimates are correct, this implies that the other important factors, such as rearrangement energies, reaction exothermicities, and aromatic group alignments, must be adjusted to a nearly optimal condition. Any departure from this optimum via, for example, a conformational change which influences the intersite distances or alignments or the rearrangement energies, could have a dramatic effect on the electron transfer rate and thus act as an electron gate. Such a capacity for gated electron flow is probably essential to the energy-conserving function of the oxidase.

Acknowledgments—We are grateful to Craig T. Martin, Jeff Gelles, and Joel Morgan for technical assistance and helpful discussions.

REFERENCES

1. Malmström, B. G. (1979) *Biochim. Biophys. Acta* **549,** 281–303
2. Beinert, H., and Palmer, G. (1964) *J. Biol. Chem.* **239,** 1221–1227
3. Chan, S. I., Bocian, D. F., Brudvig, G. W., Morse, R. H., and Stevens, T. H. (1978) in *Frontiers of Biological Energetics,* Vol. 2 (Dutton, P. L., Leigh, J. S., Jr., and Scarpa, A., eds) pp. 883–888, Academic Press, New York
4. Chan, S. I., Bocian, D. F., Brudvig, G. W., Morse, R. H., and Stevens, T. H. (1979) in *Cytochrome Oxidase* (King, T. E., Orii, Y., Chance, B., and Okunuki, K., eds) pp. 177–188, Elsevier, Amsterdam
5. Hemmerich, P. (1966) in *The Biochemistry of Copper* (Peisach, J., Aisen, P., and Blumberg, W. E., eds) p. 15, Academic Press, New York
6. Peisach, J., and Blumberg, W. E. (1974) *Arch. Biochem. Biophys.* **165,** 691–708
7. Aasa, R., Albracht, S. P. J., Falk, K.-E., Lanne, B., and Vänngård, T. (1976) *Biochim. Biophys. Acta* **422,** 260–272
8. Hartzell, C. R., and Beinert, H. (1974) *Biochem. Biophys. Acta* **368,** 318–338.
9. Sacconi, L., and Ciampolini, M. (1964) *J. Chem. Soc.* **A,** 276–280
10. Akasaka, K. (1966) *J. Chem. Phys.* **45,** 90–94
11. Hadley, J. H., Jr., and Gordy, W. (1977) *Proc. Natl. Acad. Sci. U. S. A.* **74,** 216–220
12. Castner, T. G., Jr. (1959) *Physiol. Rev.* Series 2, **115,** 1506–1515
13. Rupp, H., Rao, K. K., Hall, D. O., and Cammack, R. (1978) *Biochim. Biophys. Acta* **537,** 255–269
14. Rupp, H., and Moore, A. L. (1979) *Biochim. Biophys. Acta* **548,** 16–29
15. Lloyd, J. P., and Pake, G. E. (1953) *Physiol. Rev.* Series 2, **92,** 1576–1577
16. Fee, J. (1975) *Struct. Bonding* **23,** 1–60
17. Abragam, A., and Bleaney, B. (1970) *Electron Paramagnetic Resonance of Transition Ions,* pp. 541–583, Oxford, London
18. Kulikov, A. V., and Likhtenstein, G. I. (1977) *Adv. Molec. Relaxn. Int. Proc.* **10,** 47–79
19. Tweedle, M. F., Wilson, L. J., García-Iñiguez, L., Babcock, G. T., and Palmer, G. (1978) *J. Biol. Chem.* **253,** 8065–8071
20. Blum, H., and Ohnishi, T. (1980) *Biochim. Biophys. Acta* **621,** 9–18
21. Mailer, C., and Taylor, C. P. S. (1973) *Biochim. Biophys. Acta* **322,** 195–203
22. Orbach, R. (1961) *Proc. R. Soc. Lond. Ser. A* **264,** 458–484
23. Ohnishi, T., LoBrutto, R., Salerno, J. C., Bruckner, R. C., and Frey, T. G. (1982) *J. Biol. Chem.* **257,** 14821–14825
24. Pake, G. E. (1948) *J. Chem. Phys.* **16,** 327–336
25. Scholes, C. P., Janakiraman, R., Taylor, H., and King, T. E. (1984) *Biophys. J.* **45,** 1027–1030
26. Mascarenhas, R., Wei, Y.-H., Scholes, C. P., and King, T. E. (1983) *J. Biol. Chem.* **258,** 5348–5351
27. Wilson, M. T., Greenwood, C., Brunori, M., and Antonini, E. (1975) *Biochem. J* **147,** 145–153
28. Andréasson, L.-E., Malmström, G. B., Strömberg, C., and Vänngård, T. (1972) *FEBS Lett.* **28,** 297–301
29. Wilms, J., Dekker, H. L., Boelens, R., and van Gelder, B. F. (1981) *Biochim. Biophys. Acta* **637,** 168–176
30. Antalis, T. M., and Palmer, G. (1982) *J. Biol. Chem.* **257,** 6194–6206
31. Greenwood, C., and Gibson, Q. H. (1967) *J. Biol. Chem.* **242,** 1782–1787
32. Gibson, Q. H., and Greenwood, C. (1965) *J. Biol. Chem.* **240,** 2694–2698
33. Gibson, Q. H., and Greenwood, C. (1963) *Biochem. J.* **86,** 541–554
34. Hopfield, J. J. (1974) *Proc. Nat. Acad. Sci. U. S. A.* **71,** 3640–3644